UNIVERSITY OF ILLINOIS NUCLEAR PHYSICS LABORATORY

DESIGN OF AN 830 MEV/C OUT-OF-PLANE SPECTROMETER

S.M. Dolfini, R. Beck, L.S. Cardman, R.M. Laszewski, J.B. Mandeville, C. N. Papanicolas, S.E. Williamson
Nuclear Physics Laboratory, University of Illinois at Urbana-Champaign
Champaign, IL 61820, USA

R. Alarcon
Arizona State University
Tempe, AZ 85287, USA

M.M. Farkhondeh, J. Zumbro
Bates Linear Accelerator Laboratory
Middleton, MA 01949, USA

W. Bertozzi, W. Boeglin
Massachusetts Institute of Technology
Cambridge, MA 02139, USA

University of Illinois at Urbana Champaign

Nuclear Physics Laboratory

Department of Physics

Design of an 830 MeV/c Out-of-Plane Spectrometer

S.M. Dolfini,[1] R. Beck,[2] L.S. Cardman,[3] R.M. Laszewski, J.B. Mandeville,[4] C.N. Papanicolas,[5] S.E. Williamson
Nuclear Physics Laboratory, University of Illinois at Urbana-Champaign, Champaign, IL 61820, USA

R. Alarcon
Arizona State University, Tempe, AZ 85287, USA

M.M. Farkhondeh, J. Zumbro[6]
Bates Linear Accelerator Laboratory, Middleton, MA 01949, USA

W. Bertozzi, W. Boeglin[7]
Massachusetts Institute of Technology, Cambridge, MA 02139, USA

Abstract

We present the ion-optical and physical design of a magnetic spectrometer specifically tailored for out-of-plane coincidence (e, e′p) measurements. Four such spectrometers, together with a support system which permits them to be arrayed azimuthally about a symmetry axis in the scattering plane, comprise an out-of-plane spectrometer (OOPS) cluster. The instrument is optimized for high precision measurements on the nucleon and on few body nuclear systems.

PACS numbers: 29.30.Aj, 29.30.Ep

[1]Current address; Arizona State University, Tempe, AZ 85287, USA.
[2]Current address; University of Mainz, Mainz, Germany.
[3]Current address; Continuous Electron Beam Facility (CEBAF), Newport News, VA 23606 USA
[4]Current address; Massachusetts General Hospital, Charlestown, MA, 02129 USA.
[5]Current address; National and Capodistrian University of Athens, GREECE.
[6]Current address; Los Alamos Meson Physics Facility (LAMPF), Los Alamos, NM 87544, USA.
[7]Current address; University of Mainz, Mainz, Germany.

1 Introduction

Coincident out-of-plane particle detection can provide important information about several very interesting but relatively small components of the electron scattering cross section [1]–[5]. Consequently, a number of schemes for the detection of high-momentum charged particles out of the scattering plane have been proposed for use at new cw electron accelerator facilities [6]–[10]. In particular, a dedicated out-of-plane detection system for high precision experiments on light nuclei is currently under construction at the Bates Linear Accelerator Center. This system consists of a support structure and four independent magnetic spectrometer modules that can be arrayed azimuthally about a symmetry axis located in the scattering plane. The Out-of-Plane Spectrometer (OOPS) system is designed to be used with an in-plane electron spectrometer, such as OHIPS at Bates, to measure coincident $(e, e'p)$ cross sections simultaneously at four angles. Simultaneous four-fold measurements permit the extraction of important nuclear structure information from asymmetries in the relative coincidence cross sections [3]. Absolute cross-section determinations are not required. In addition, this Separation Through Asymmetries Method (STAM) substantially reduces the magnitude of certain systematic errors. When azimuthally symmetric detector placement is precluded or is undesirable, the OOPS system allows for independent asymmetric positioning of the individual spectrometer modules.

In the present report we describe the ion-optical and physical design of a spectrometer module that has been specifically tailored for out-of-plane applications. In section 2 a number of theoretical, experimental and physical considerations that constrain the design are discussed. The optical design of the spectrometer is presented in section 3, and the physical configuration is described in section 4. Important issues regarding alignment tolerances and their bearing on performance are treated in section 5. The measured performance characteristics of a prototype module are reported in a companion paper [11].

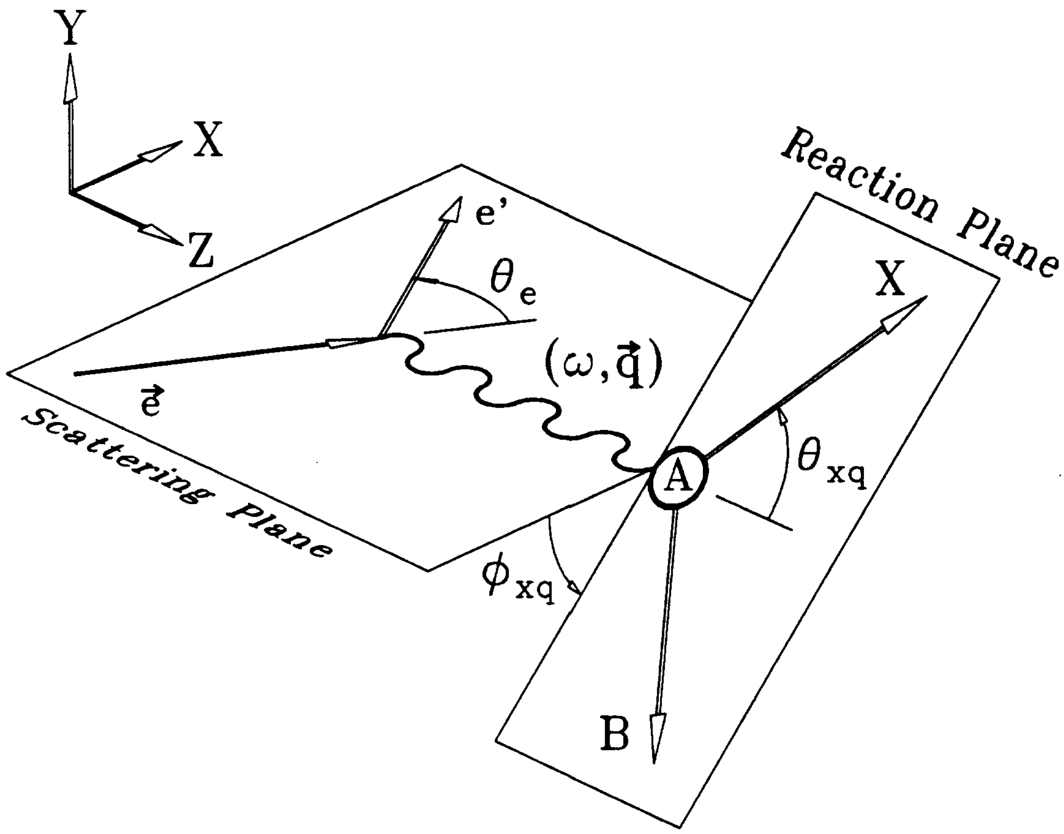

Figure 1: Kinematic definitions for the A(e, e'x)B reaction.

2 Spectrometer Design Considerations

The kinematics of the coincident electron scattering reaction A(e, e'x)B are illustrated in Figure 1. The scattered electron emits a virtual photon in the momentum transfer direction, $\vec{q}$, which interacts with the nucleus transferring to it momentum $\vec{q}$ and energy ω. The decay product x is detected at a polar angle θ_{pq} and an azimuthal angle ϕ_{pq} relative to the momentum transfer direction. The cross section for this reaction in Plane Wave Born

Approximation is [10]:

$$
\begin{aligned}
d\sigma(q,\omega) \;\propto\; & d\sigma_{Mott}\{U_L R_L(q,\omega) + U_T R_T^+(q,\omega) \\
+ \; & U_{TT}[\cos 2\phi_{pq} R_{TT}(q,\omega) + \sin 2\phi_{pq} \tilde{\mathbb{R}}_{TT}(q,\omega)] \\
+ \; & U_{TL}[\cos \phi_{pq} R_{TL}^-(q,\omega) + \sin \phi_{pq} \tilde{\mathbb{R}}_{TL}^+(q,\omega) \\
+ \; & hU'_{TL}[\cos \phi_{pq} \mathbb{R}_{TL}^+(q,\omega) + \sin \phi_{pq} R_{TL}^-(q,\omega)] \\
+ \; & hU'_T \mathbb{R}_T^-(q,\omega)\} \quad .
\end{aligned} \tag{1}
$$

where $d\sigma_{mott}$ is the cross section for scattering from a point charge, and the U's are kinematic factors. The beam helicity is denoted by h. All of the nuclear structure information is contained in the responses, R and $\mathbb{R}$, which are bilinear functions of the nuclear transition current.

The $\mathbb{R}$-functions can only be observed in experiments which employ a polarized target or are sensitive to recoil polarization, and a discussion of methods for their determination is beyond the scope of this report. However, equation 1 shows that if out-of-plane measurements can be made with detectors placed at integer multiples of $\pi/4$ in ϕ_{pq} it is possible to extract the responses R_{LT}, R_{TT}, and R'_{LT} from the coincident electron scattering cross section with maximum sensitivity. Asymmetry ratios that are proportional to the response functions can be formed between various combinations of measurements at $n \cdot \frac{\pi}{4}$ [3]. Four out-of-plane detectors can be placed symmetrically either at $n \cdot \frac{\pi}{2}$ corresponding to a '+'-configuration, or at $(n + 1/2) \cdot \frac{\pi}{2}$ corresponding to an 'x'-configuration. These orientations are shown schematically in Figures 2 and 3. We note that, in conjunction with Rosenbluth separation techniques, such a four-spectrometer out-of-plane system would permit the isolation of all of the response functions that are observable in coincident electron scattering. A more detailed discussion of the STAM technique and its advantages with regard to the control of systematic errors can be found in references [3, 9].

The ion-optical characteristics of a useful out-of-plane spectrometer must meet a set of performance criteria that were developed in the course of preparing proposals for the first

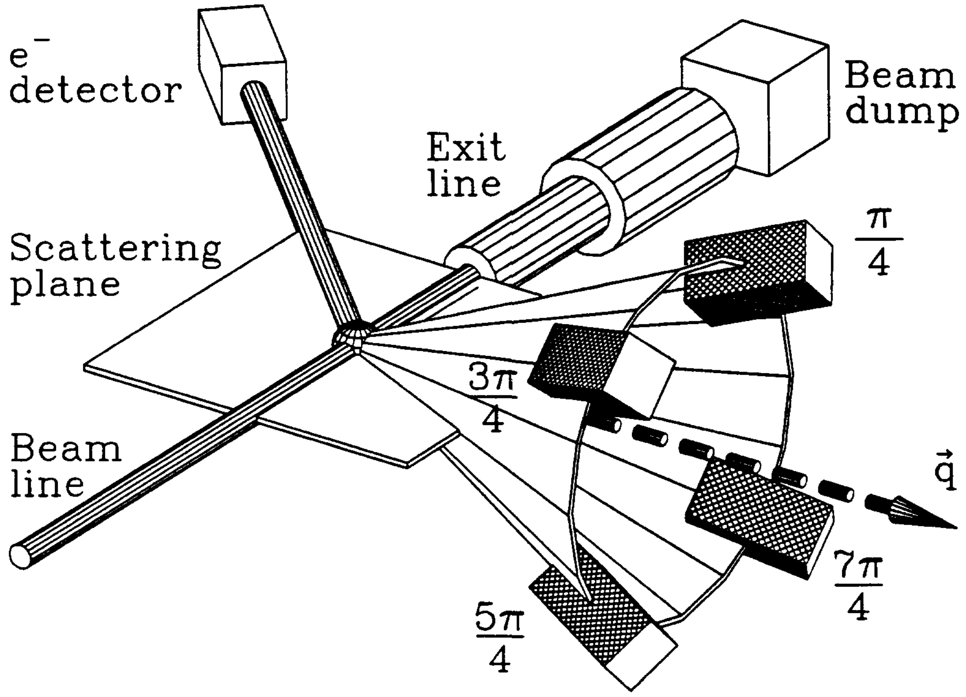

Figure 2: Schematic representation of the experimental geometry in the 'x'-configuration.

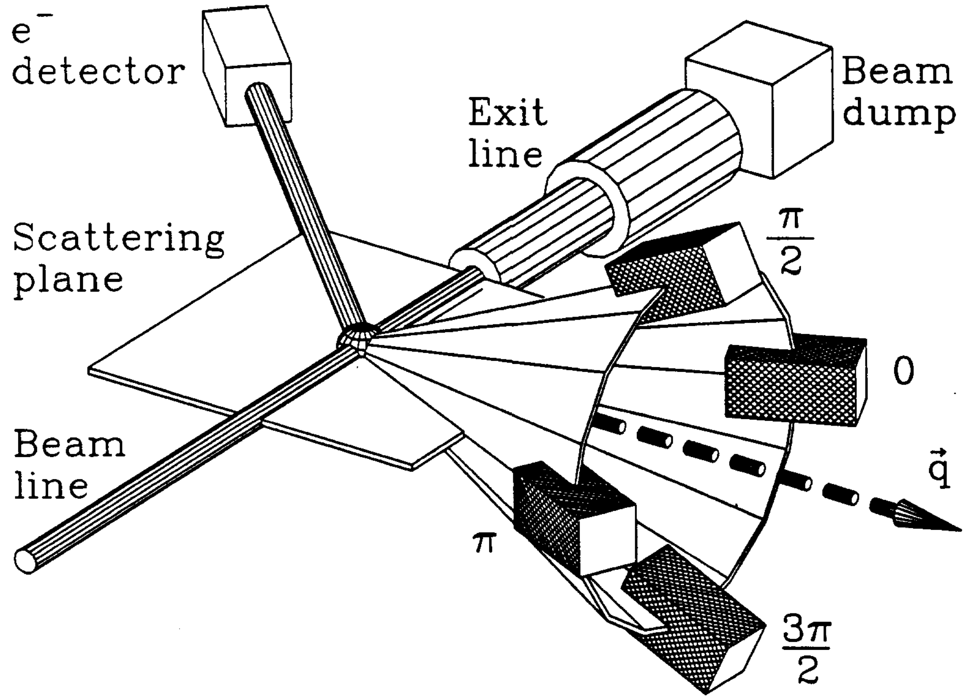

Figure 3: Schematic representation of the experimental geometry in the '+'-configuration.

of out-of-plane experiments at Bates [12]–[14]. A careful review of this work shows that a reasonable design consistent with the experimental objectives and the kinematic regions that are accessible at Bates will have:

1. Momentum resolution: $\lessapprox 1 \times 10^{-2}$.

2. Angular resolution: $\theta_{\mathbf{pq}}$, $\phi_{\mathbf{pq}} \lessapprox 5$ mr.

3. Angular acceptance: $\gtrapprox 2$ msr per module.

4. Maximum momentum: $\gtrapprox 600$ MeV/c.

As will be discussed in sections 3 and 5 the final design was able to meet or exceeded criteria (1), (2), and (4). However, the angular acceptance was ultimately limited to about 1.2 msr because of a decision to use available surplus magnets as a cost consideration. We note that a spectrometer of the type discussed in this paper could achieve a solid angle exceeding 4 msr if specially designed magnets were employed.

Geometrical constraints put severe restrictions on the angular ranges that are accessible to real out-of-plane asymmetry measurements. The individual spectrometer modules can interfere with each other and with various obstacles in the experimental hall. The physical interference problem is exacerbated because it is often necessary for the symmetry axis of the OOPS system to be oriented along the momentum transfer vector of the reaction. The direction of this vector is always in the forward direction, and in many cases it can lie at small angles with respect to the beam direction.

Small values of the opening angle $\theta_{\mathbf{pq}}$ are generally limited by the mutual interference between modules. At large $\theta_{\mathbf{pq}}$, the beam exit line, the collateral electron spectrometer, and the floor of the experimental hall can all restrict the location of modules. In an environment such as that of the south experimental hall at Bates, where the beam-line height and the size of the secondary electron spectrometer are predetermined, the physical size and weight of the individual OOPS modules must be kept to a minimum consistent with ion-optical design and cost considerations. In order to allow for a trade-off between the minimum value of θ_{pq} and the maximum angular acceptance, it is desirable to retain the option of operating the spectrometers at varying distances from the target.

3 Optical design

As a cost consideration, the design of the out-of-plane spectrometer module makes use of surplus magnets. It was possible to obtain suitable dipole magnets from Fermilab and quadrupole magnets from Brookhaven National Laboratory. A dipole-quadrupole (DQ) configuration was found to be the most practical alternative for our out-of-plane applications. Because of the greater relative bulk of the quadrupole, the DQ orientation helps to achieve minimum interference between adjacent modules at small θ_{pq}. This point is illustrated in Figure 4 which shows a of cluster of four (DQ) OOPS modules as they will appear in the south hall at Bates. The spectrometers are in shown in the 'x'-configuration.

The surplus dipole magnets were originally intended for the Fermilab Cooling Ring experiment [15]. These magnets were designed to work in the ring environment and operate at a nominal magnetic field of 4.3 kG. The dipole is a modified picture frame magnet with a Rose shim that extends the flat field region to within 1/2 gap-length of the coil. There is a non-uniformity in the field at the level of 1–2 parts in 10^4 over the 20.3 cm pole-width. The dimensions and characteristics of this magnet are summarized in Table 1. The Fermilab dipole magnets have a very narrow profile which makes them particularly useful for close-packed applications.

The magnetic field characteristics of the dipole magnets were investigated with the 2-dimensional code POISSON [16]. It can be seen from Figure 5 that the magnet just begins to saturate at an excitation of 6.0 kG. Field maps for peak values of 4.3 kG and 8.0 kG are shown in Figure 6. At 8.0 kG the magnet is in saturation, but the field in the gap remains

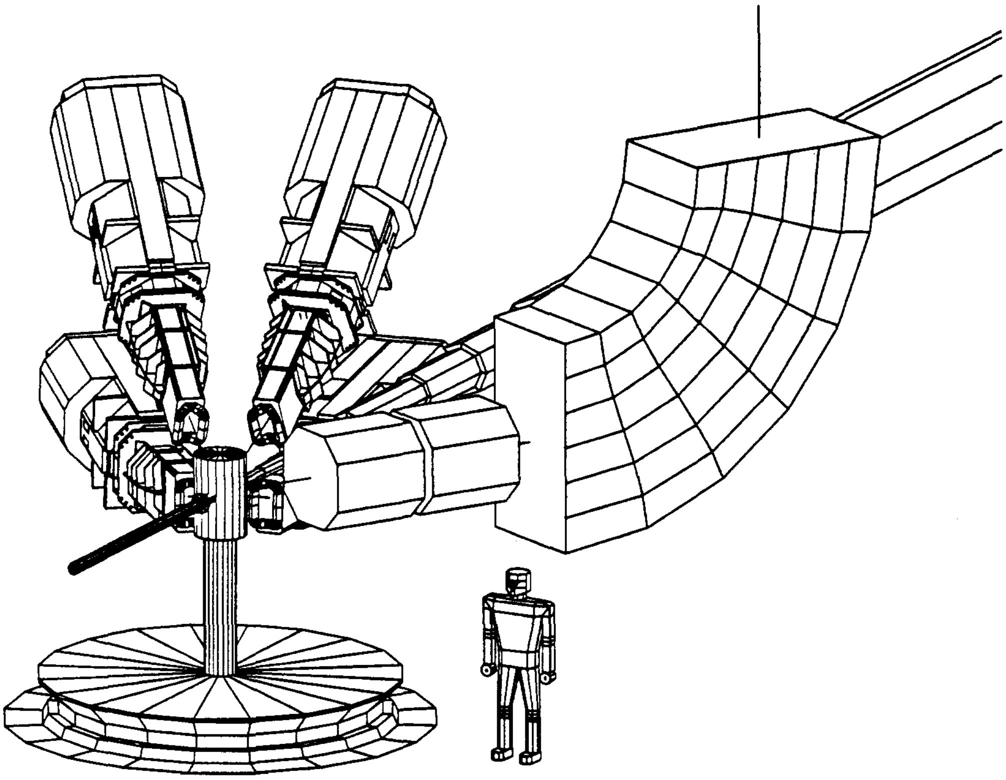

Figure 4: Typical arrangement of a cluster of four OOPS spectrometers with an in-plane electron spectrometer.

relatively flat. A measured field flatness curve for a peak field of 4.3 kG is also shown in Figure 7 [15]. This curve lies close to the POISSON prediction.

The surplus quadrupole magnets from Brookhaven are 61 cm long and have 20 cm bores. These magnets can achieve a maximum pole tip field of 11 kG. The quadrupole magnet specifications are listed in Table 2. Excitation curves for the quadrupole magnets were measured by the Pacific Motor Company [17], by the T_{20} collaboration [18] and by our group. All of the results are summarized in Figure 8.

As was noted in section 2, the optical design of the OOPS module is constrained by a number of factors related to overall physical bulk as well as to the angular acceptance and momentum resolution demands on the spectrometer. In order to achieve the best compromise between

Field Strength	4.3 kG
Magnet length	48 in.
Cross section dimensions	10 in. by 22 in.
Magnet effective length	51.52 in.
Magnet gap	3.25 in.
Coil Aperture	12 in.
Field Aperture	±4.00 in.
Field quality ($\Delta B/B$ within 3 in.)	$\pm 10^{-4}$
Conductor current	711 A
Coil resistance	0.025 Ω
Magnet weight (approx.)	2388 lb

Table 1: Dipole magnet specifications [15].

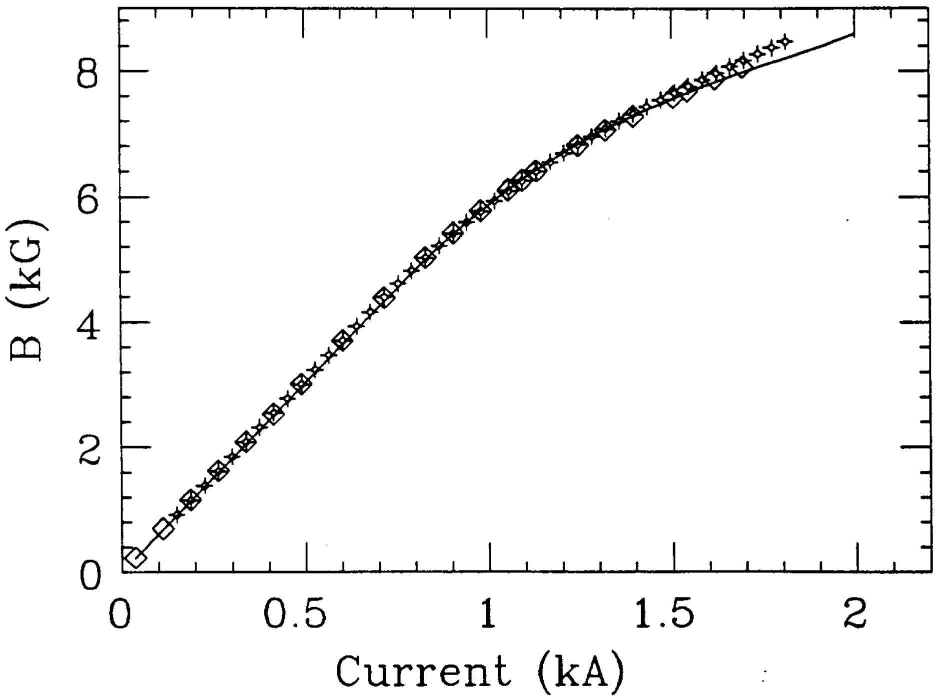

Figure 5: The OOPS dipole magnet excitation curves. The diamond and star points represent measurements from two different dipole magnets. The solid curve represents a 2-dimensional POISSON [16] calculation.

the solid angle and the range of accessible angles θ_{pq}, an initial drift distance of 1.4 meters was

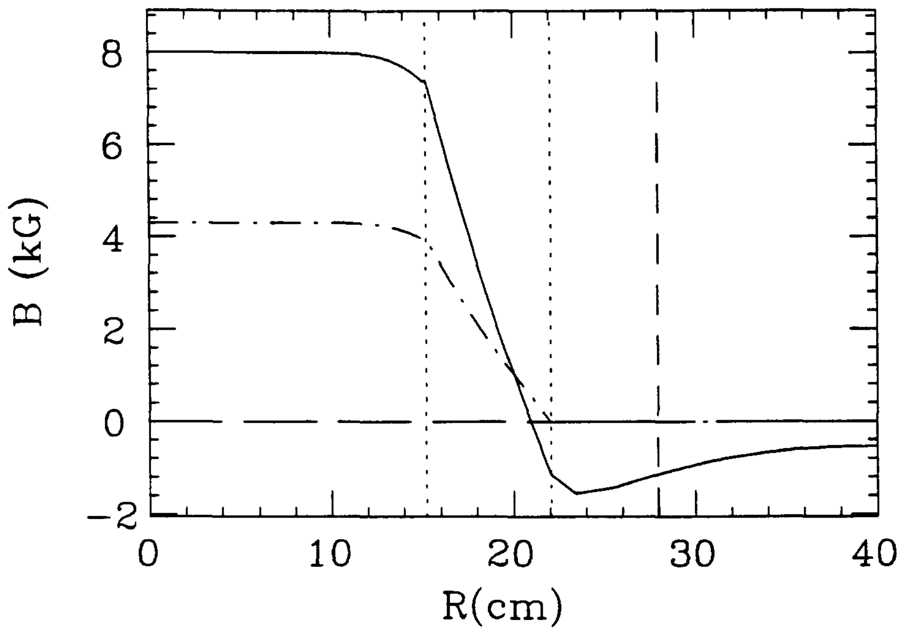

Figure 6: Field maps for the dipole magnet calculated with POISSON. The solid and dash-dot curves represent calculations at 8.0 and 4.3kG, respectively. The dot, dash and long dash curves represent the coil boundaries, the magnet boundary and the zero line, respectively.

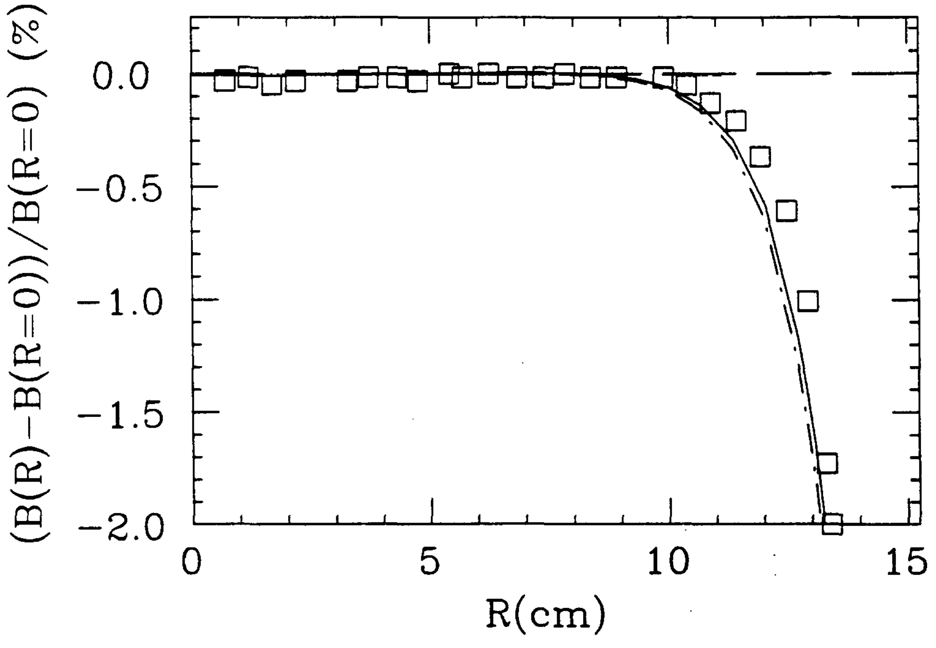

Figure 7: Field flatness curves for the dipole magnet calculated with POISSON. The solid and dash-dot curves represent calculations at 8.0 and 4.3kG, respectively. The Fermilab measurement of field flatness [15] presented as square points, is shown for comparison. The long dash curve is the zero line.

Field Strength	11.0 kG
Magnet length	24 in.
Cross section dimensions	35 in. by 35 in.
Magnet bore	8.0 in.
Conductor current	500 A
Coil resistance	0.4 Ω
Magnet weight (approx.)	5800 lb

Table 2: Quadrupole magnet specifications [17].

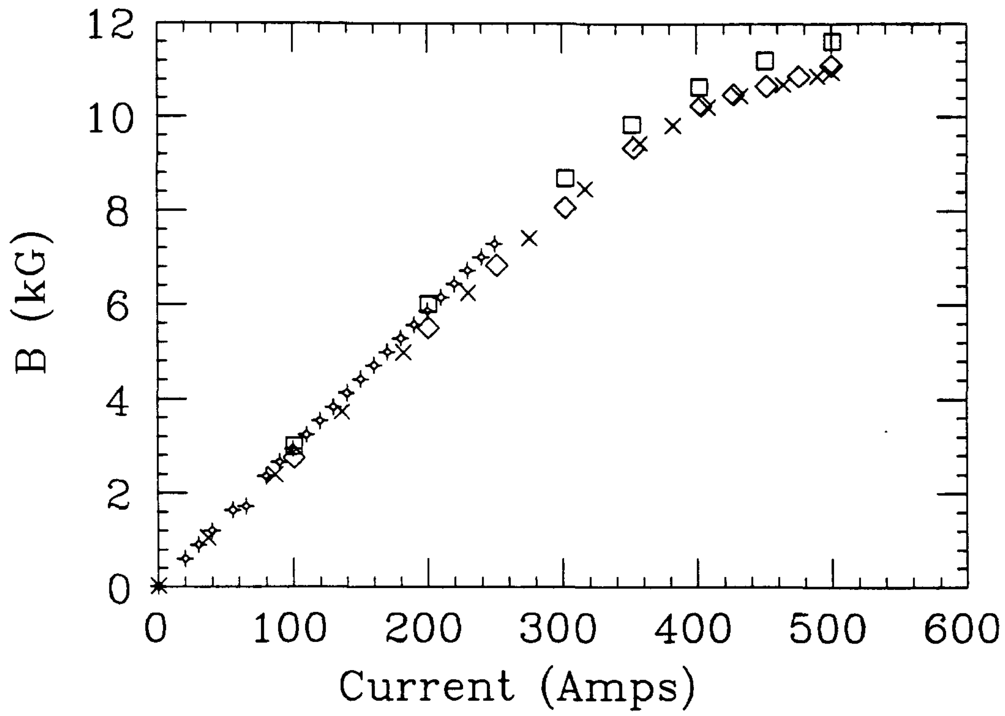

Figure 8: The OOPS quadrupole magnet excitation curves. The diamond and square points represent measurements of two different quadrupole magnets by the T_{20} collaboration [18]. The star points represent a measurement of one quadrupole magnet by our group. The cross points represent a measurement by the Pacific Motor Company [17].

chosen. At this distance the dipole magnet alone would have a virtual focus in momentum. The quadrupole magnet is required to generate a useful focal surface.

Several DQ configurations with different bend angles were explored. Larger bends can provide better momentum resolution at the cost of a reduction in the maximum momentum.

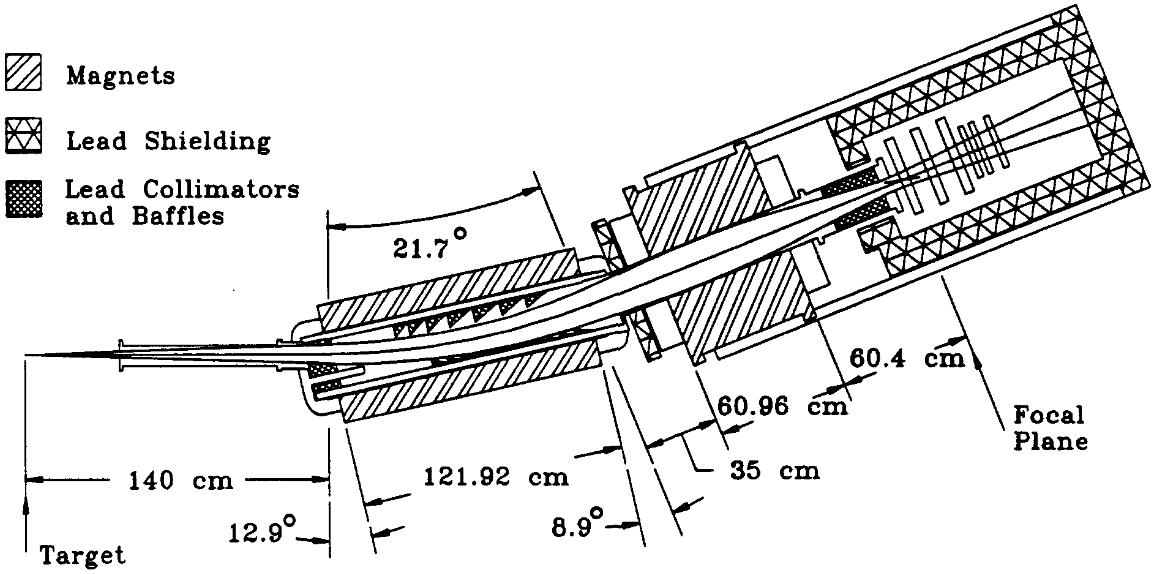

Figure 9: A cross sectional elevation of the OOPS module. The key elements of the spectrometer are drawn to scale.

A reasonable compromise design that can accommodate the resolution demands of the out-of-plane experiments was found to have a maximum central momentum of 830 MeV/c (at 8.0 kG) and a bend of 21.7°. An alternative higher-resolution configuration, with a maximum momentum of 625 MeV/c and a bend of 29.0° was also studied in some detail. For completeness, both the reference high-momentum design and the alternative high-resolution design are summarized in Tables 3.

The conceptual design of the instrument was established with TRANSPORT [19]. RAYTRACE [20, 21] and TURTLE [22] were used to optimize the focal plane optics and the momentum and angular acceptances of the spectrometer. A cross section of the layout of the OOPS module in the high-momentum configuration is shown in Figure 9. The effective length of the dipole magnet is 130.9 cm [15], and the effective length of the quadrupole magnet is 69.2 cm.

The beam envelope as well as some of the more important transfer matrix elements are shown in Figure 10 over the length of the spectrometer. The momentum resolution is 0.25 % for a target size of ± 0.1 cm, and the angle of the focal plane relative to the central trajectory is

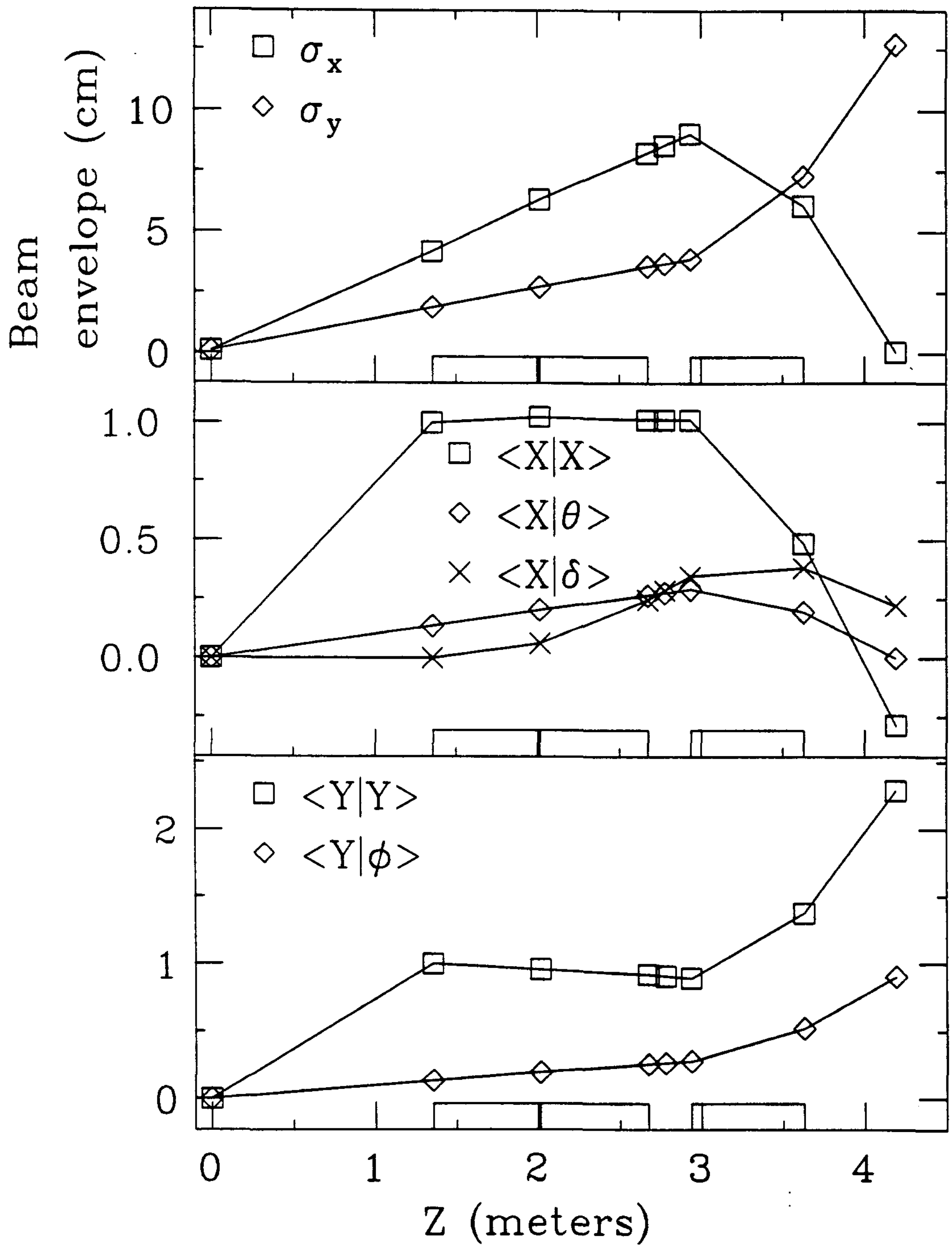

Figure 10: TRANSPORT variables along the spectrometer. Blocks along each abscissa indicate the placement and length of magnetic elements.

Design	High Momentum	High Resolution
Geometry	DQ	DQ
Max. central momentum	832.8 MeV/c	625.0 MeV/c
Solid angle	1.2 msr	
Angular opening	±25.0 x ±12.0 mr	
Initial drift distance	1.40 m	1.40 m
Entrance pole face rotation	12.86°	17.00°
Dipole field	8.00 kG	8.00 kG
Exit pole face rotation	8.86°	12.00°
Total bend angle	21.72°	29.00°
Bend radius	3.47 m	2.60 m
Dipole-Quadrupole distance	0.35 m	0.35 m
Quadrupole field	6.74 kG	5.05 kG
Quadrupole radius	10.16 cm	10.16 cm
Final drift distance	0.60 m	0.60 m
Total distance	4.19 m	4.19 m

Table 3: Comparison of OOPS module physical characteristics for two DQ configurations

12.7°. Table 4 presents a summary of the optical characteristics of both the high-momentum OOPS design and the alternate high-resolution option.

The measured fringe fields shown in Figures 11 and 12 [23] were used in the RAYTRACE computations. Field measurements of the dipole magnet were made for peak fields of 3.0, 6.0 and 8.0 kG, and of the quadrupole magnet for fields of 3.8 and 5.2 kG. It can be seen from the figures that the fringe field profiles change only slightly with variations in field strength over these ranges.

The focal surface was found to be nearly flat, lying at an angle of 12.9° relative to the central trajectory. This result is consistent with that obtained from the TRANSPORT calculations. The momentum resolution of the spectrometer as a function of δ, and the angle, ϕ_{target}, is shown in Figure 13. It can be seen that the intrinsic momentum resolution of the spectrometer exceeds the design target of 1×10^{-2} over the full range of momentum acceptance.

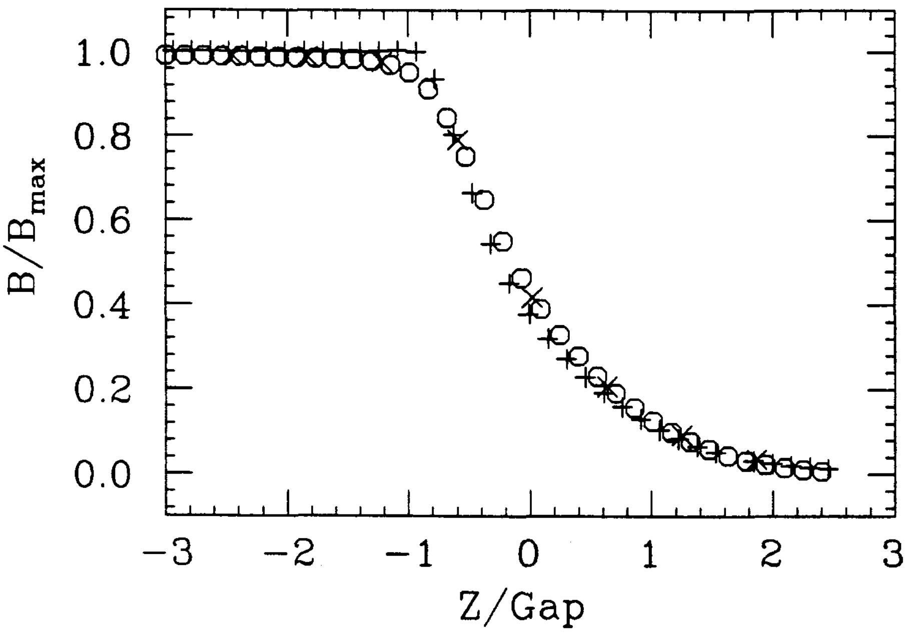

Figure 11: The measured fringe field of the dipole magnet. The circle, cross and plus points represent maximum magnetic fields of 8.0, 6.0 and 3.0 kG, respectively.

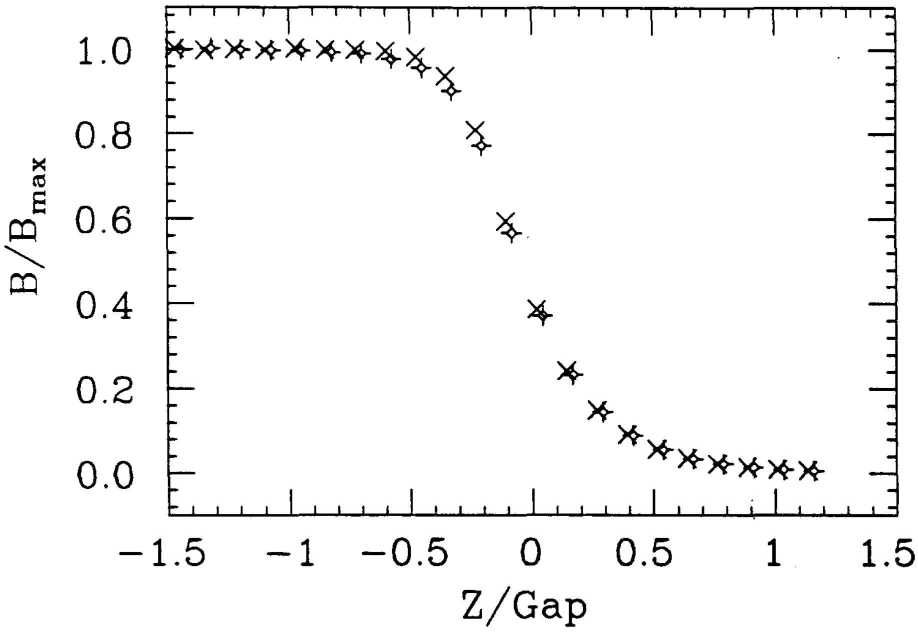

Figure 12: The measured fringe field of the quadrupole magnet. The plus and cross points represent maximum magnetic fields of 5.18 and 3.75 kG, respectively.

Design	High Momentum	High Resolution
Optics	Point to point in Dispersive plane	Point to point in Dispersive plane
"Flat" momentum bite	10.0 %	
Focal plane length	16.3 cm	16.4 cm
Focal plane width	24.0 cm	23.9 cm
Focal plane angle	12.7°	17.4°
$\delta P/P(\times 10^2)$:		
$\delta = -8\%$	0.44	
$\delta = 0\%$	0.35 (0.25)[a]	(0.19)
$\delta = +8\%$	0.53	
1^{st} order matrix elements:		
$\langle x\|x\rangle$	-0.29	-0.29
$\langle x\|\theta\rangle$	0.00 cm/mr	0.00 cm/mr
$\langle x\|\delta\rangle$	0.22 cm/%	0.30 cm/%
$\langle \theta\|x\rangle$	-13.74 mr/cm	-13.85 mr/cm
$\langle \theta\|\theta\rangle$	-3.49	-3.47
$\langle \theta\|\delta\rangle$	-2.88 mr/%	-3.82 mr/%
$\langle y\|y\rangle$	2.29	1.94
$\langle y\|\phi\rangle$	0.91 cm/mr	0.85 cm/mr
$\langle \phi\|y\rangle$	16.21 mr/cm	13.39 mr/cm
$\langle \phi\|\phi\rangle$	6.86	6.39

[a]The resolutions in parenthesis are derived from TRANSPORT. Others are from RAYTRACE.

Table 4: Comparison of OOPS module optical characteristics for two DQ configurations

The orientation angle of the focal plane has important consequences for the choice of an appropriate detector package. If the focal plane angle is appreciable ($\gtrsim$ 20°) then Vertical Drift Chambers (VDC) can be used to determine focal plane coordinates. Typically, VDC's are mounted along the focal plane and yield the momentum spectrum directly. With a focal plane angle as flat as 12.9°, however, the windows of a VDC would introduce too much multiple scattering and degrade the resolution. In this case, Horizontal Drift Chambers (HDC) [24]–[26] are a better choice in that they can be mounted perpendicular to the central ray. This minimizes the possibility of multiple scattering, but at least two HDC's are required in order to to reconstruct particle trajectories at the focal plane.

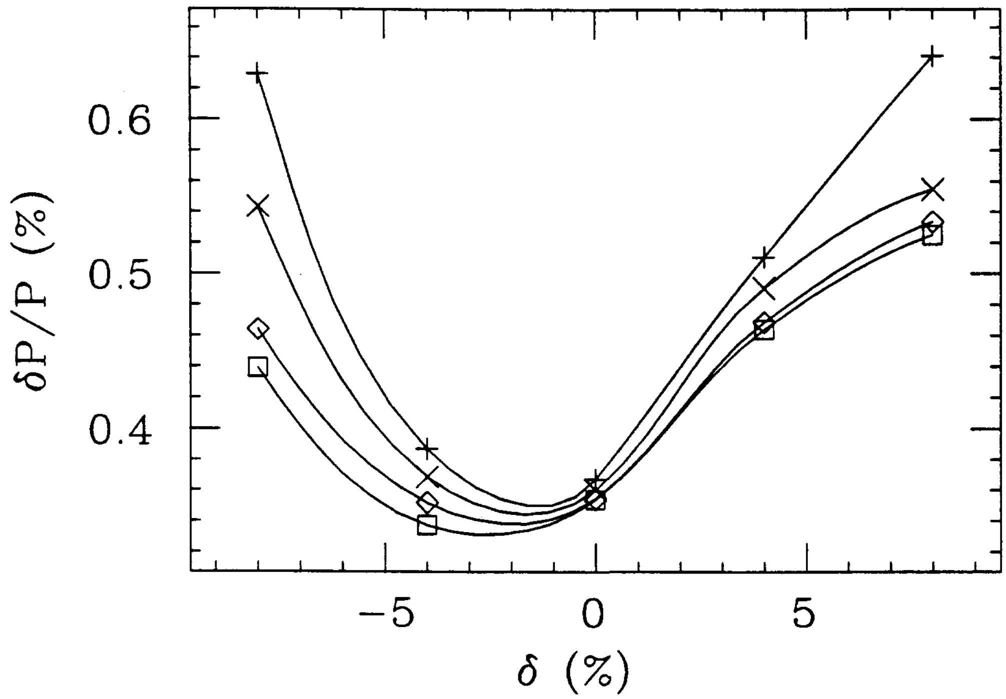

Figure 13: Focal plane momentum resolution as a function of δ and $\phi_{\mathbf{target}}$. The Plus, cross, diamond and square points represent resolutions calculated for $\phi_{target} = \pm 12$, ± 4, and 0 mr, respectively.

The acceptance and the extended target efficiency of the spectrometer were studied with TURTLE. Collimators and other physical obstructions were included in order to create as realistic a representation of the optical system as possible. The acceptance profile of the spectrometer is shown in Figure 14. It can be seen that as the dispersion-plane angle $\theta_{\mathbf{target}}$ is reduced from ± 25 to ± 20 mr, the range over which the detection-efficiency is flat increases. For an angular acceptance of ± 20 mr, the efficiency is uniform over a momentum acceptance bite of about 16%. The detection efficiency for particles coming from an extended target is shown in Figure 15. As the angular acceptance in the non-dispersion plane, $\phi_{\mathbf{target}}$ is restricted, the efficiency remains flat over longer targets. A reasonable acceptance of $\theta_{\mathbf{target}} = \pm 25$ mr and $\phi_{\mathbf{target}} = \pm 12$ mr would correspond to a solid angle of about 1.2 msr. This angular acceptance falls somewhat below the design target of 2 msr, but it is about as large as can be obtained with the present dipole magnet while retaining a reasonable minimum value for the opening angle θ_{pq}. At 1.4 m drift distance θ_{pq} can be as small as 20.5° in the '+'-configuration and 16.3° in the 'x'-configuration.

Because smaller opening angles θ_{pq} can be achieved by increasing the initial drift distance from the target, it is of interest to consider the effect that backing away has on the optics of the spectrometer. As the initial drift distance is increased, the quadrupole field must be lowered at a rate of 0.39 kG/m in order to keep the nominal focal surface at the location of the physical focal plane detectors. At the same time, the pitch of the focal plane relative to the central trajectory increases at a rate of approximately 2.0°/m. The momentum resolution improves slowly at about 0.07%/m. Less desirably, the solid angle drops as the inverse square of the target distance.

4 Physical Configuration

The physical layout of an OOPS module is shown in Figure 16. The spectrometer is about 4 m long, 1.2 m wide at the widest point, and weighs about 15,000 kg. At the rear of the spectrometer is an octagonal support tube that surrounds the detector package. This tube is constructed from 5 cm thick welded plate steel, and incorporates 4 beams that extend forward to grasp the quadrupole magnet. The tube also supports a 15 cm-thick layer of lead shielding for the detectors. Two trunnions are located close to the center of gravity of the spectrometer and extend horizontally from the octagonal tube. They can bear the entire weight of the spectrometer. The quadrupole magnet is attached in turn to the dipole magnet by means of a dipole-quadrupole interface support and a dipole support clamp. The dipole-quadrupole interface support is used as a spacer for correct positioning of the dipole magnet and also holds a lead plate forward of the quadrupole magnet for shielding. The dipole clamp is attached to the interface support. It is constructed of two rigid stainless steel plates that lie on either side of the dipole magnet. Accurate positioning of the dipole magnet is achieved with shims placed between the magnet and the fixed sides of the dipole

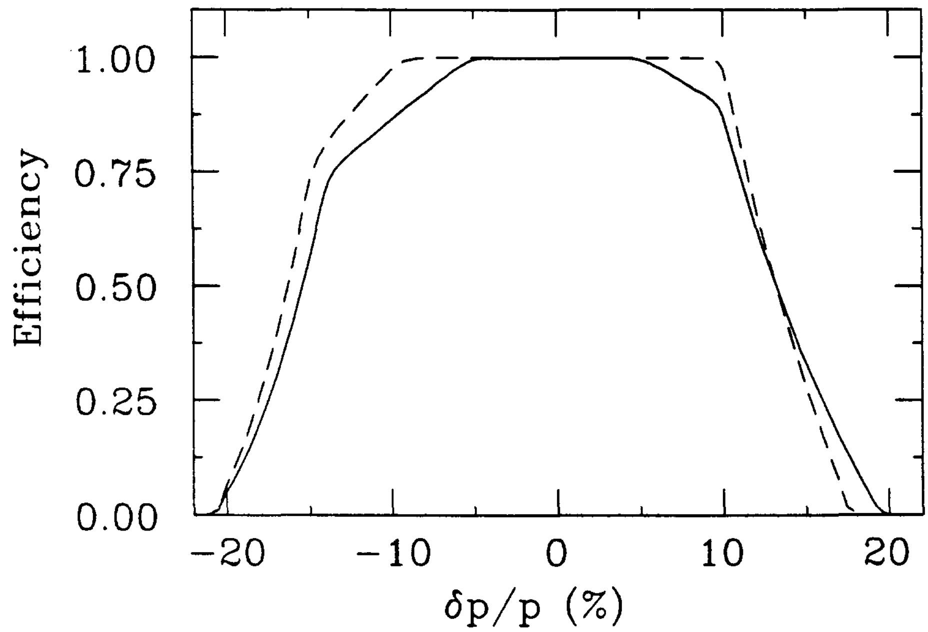

Figure 14: Momentum acceptance profile. The solid and dashed curves represent θ_{target} acceptances of 50 mr and 38 mr, respectively.

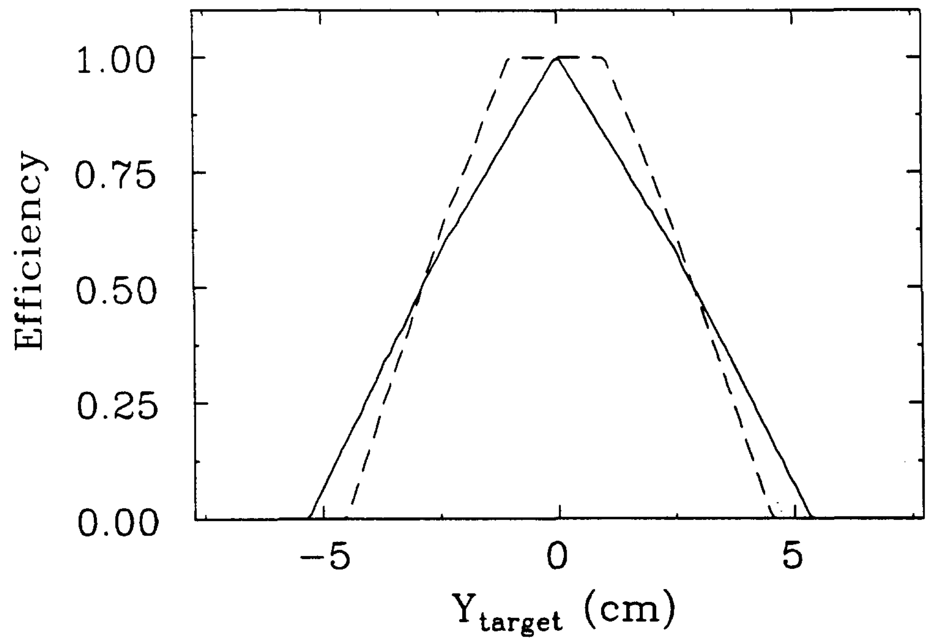

Figure 15: Extended target acceptance profile. The solid and dashed curves represent ϕ_{target} acceptances of 24 mr and 16 mr, respectively.

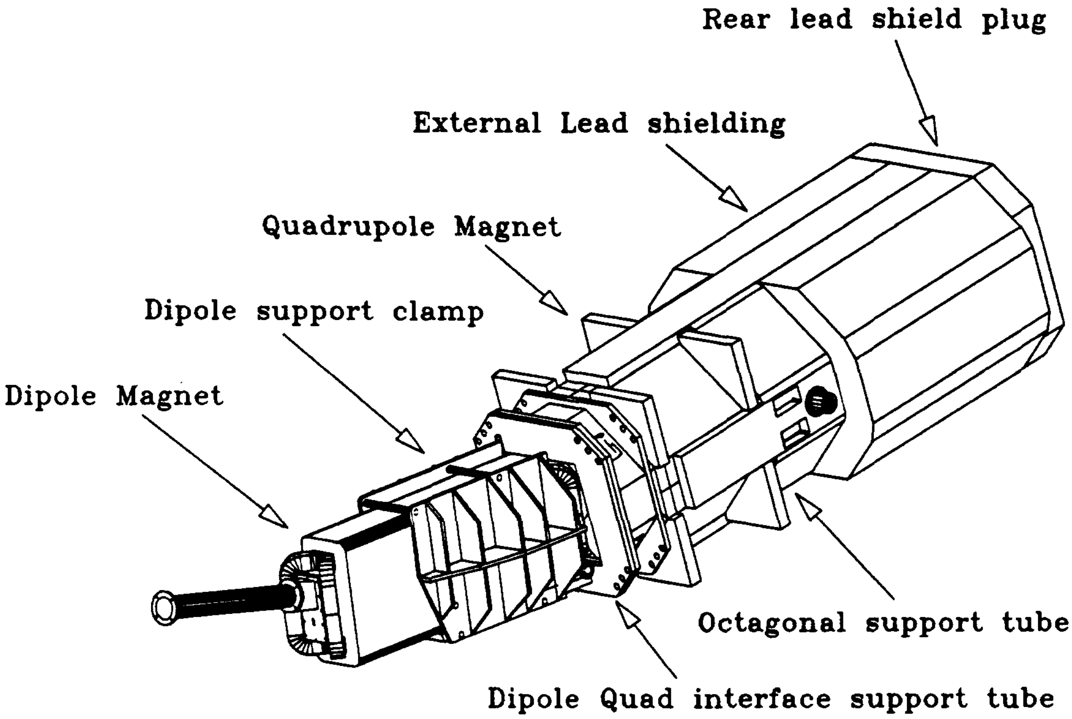

Figure 16: Components of the OOPS module.

clamp. We note that the modular nature of the dipole magnet support-structure provides for the possibility of rebuilding the spectrometer in the high-resolution configuration discussed above if it becomes desirable to do so in the future.

Spectrometers of this design can be nested closely together. If the spectrometers are placed around the target with an initial drift distance of 1.4 meters, the minimum separation in the horizontal plane is 20.5° and in the vertical plane 23.0°. Figure 14 illustrates the way in which these values translate into minimum symmetric opening angles. For the 'x'-configuration, $\theta_{pq} > 16.3°$, and for the '+'-configuration, $\theta_{pq} > 20.5°$. In the Bates South-Hall environment the target height is 2.1 m, and an OOPS spectrometer can be lowered below the reaction plane to an angle of about 32.4°. This implies that the maximum opening angle in the '+'-configuration is 32.4°. In the 'x'-configuration, this angle can be as large as 45.8°. If the drift distance is increased to achieve smaller θ_{pq}, the maximum θ_{pq} will be reduced.

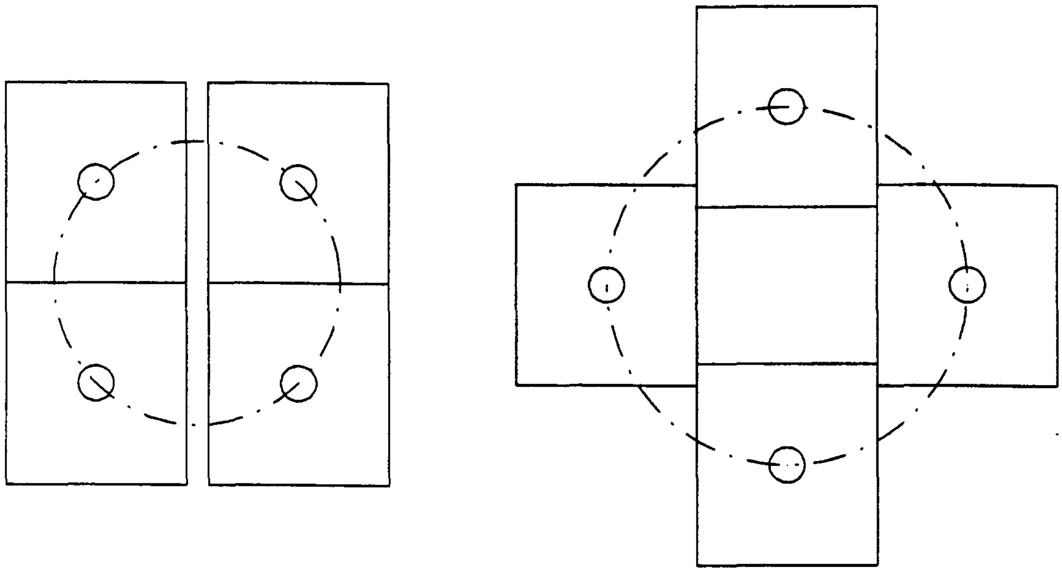

Figure 17: Schematic end-on view of the OOPS cluster showing the spectrometers in the 'x' (θ_{pq} = 16.3°) and '+' (θ_{pq} = 20.5°) -configurations, respectively. The dot-dash line represents the minimum cone of protons that can be detected symmetrically with an initial drift distance of 1.4 m.

The OOPS module vacuum system is shown in Figure 18. It is composed of five main pieces, all of which are constructed of non-magnetic stainless steel. O-rings form the seal between the components, and support a vacuum of better than 1×10^{-3} torr. The snout extension pipe connects the spectrometer vacuum to that of the scattering chamber. Normally it terminates in a 0.013 cm (5 mil) kapton window, but a direct connection to the scattering chamber vacuum is also possible. The snout piece fixes the angle of the snout extension pipe, and can hold both a sieve slit for calibration purposes, and an NMR probe for measuring the magnetic field of the dipole magnet. The dipole vacuum box extends through the dipole magnet. It has a pump-out port, and supports the solid-angle-defining collimator and a system of baffles. This vacuum box is aligned and fixed rigidly to the dipole magnet. The quadrupole vacuum box extends through the quadrupole magnet, supports a ring collimator, and has a small bellows near the dipole vacuum box to permit relative alignments. The quadrupole vacuum box extension makes the connection to the detector system. It holds a

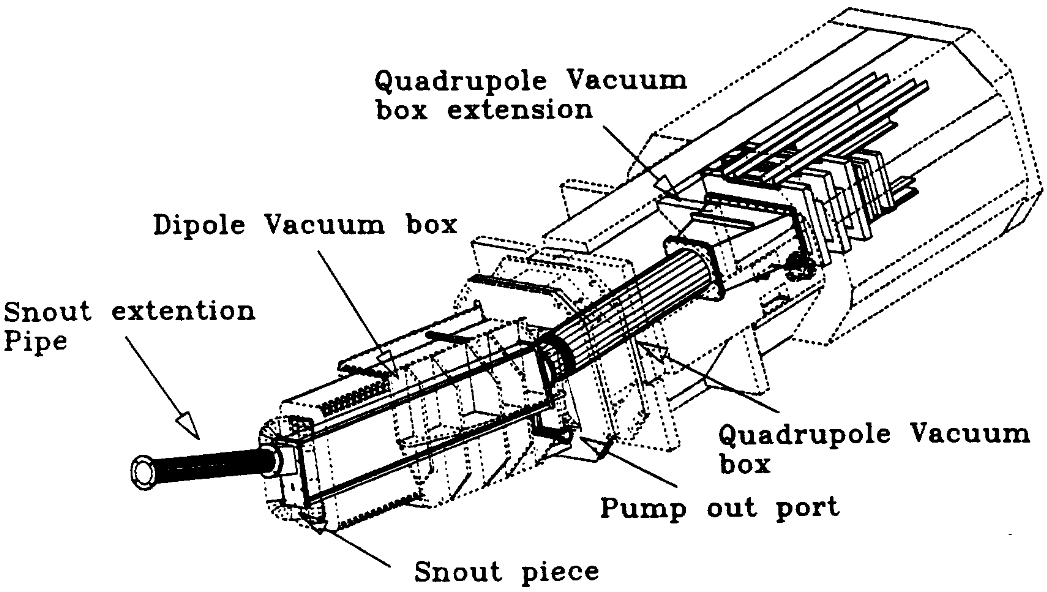

Figure 18: A view of the OOPS module vacuum and detector systems positioned within the spectrometer.

140 kg momentum-defining collimator, and terminates in an exit plate with a 0.013 cm-thick kapton window.

Shielding of various kinds is necessary to protect the particle detectors and associated electronics from the intense background radiation of the experimental hall. Shielding for the OOPS module is fairly straightforward. Particle trajectories are bent sufficiently so that there are no line-of-sight paths through the magnetic elements from the target to the focal plane. The system of collimators and baffles, shown in Figure 19, defines the spectrometer solid angle and reduces the number of particles that are scattered at small angles within the dipole magnet. At the entrance of the spectrometer, a 13 cm-thick lead collimator is used to define the angular acceptance. This collimator is mounted inside the dipole vacuum box flush with the vacuum flange. It subtends a maximum opening of $\pm 31 \times \pm 11$ mr at a drift distance of 1.4 m. Inserts can be placed in this collimator to define the acceptance. A ring collimator is mounted between the dipole and quadrupole magnets. This collimator is used to reduce the spread of particles in the bend plane so that small angle scattering will not occur in the quadrupole magnet. It is 6.4 cm long and has a radial thickness of 1.3 cm. The rear collimator lies between the quadrupole magnet and the entrance to the detector system. It is designed to reduce the momentum spread of particles entering the detector system. In both the dispersive and transverse planes, the interior of this collimator is tapered to conform to the envelope of rays entering the detector system. The rear collimator also serves as part of the shielding for the detector system by filling much of the space between the quadrupole magnet and the detectors. It weighs 140 kg and is 26.0 cm long.

The focal plane detectors are attached to a carriage which is mounted on linear bearings that are fastened to the inside of the octagonal support tube. These bearing rails facilitate accurate and easy removal and installation of the detector system. The rails employed in this system support the detector package at any orientation of the OOPS module. The detector system is shielded by the 5 cm of steel that make up the octagonal support tube as well as by 15 cm of lead mounted around the tube. Additionally, there are 13 cm of lead making up a rear door, and 13 cm of lead inside the support tube, between the detector system and the quadrupole magnet.

The optical focal-plane of the OOPS module is not quite a flat surface, and it lies at a very shallow angle with respect to the central ray (see Table 4). Three crossed wire HDC's are used to track particles passing through the focal region of the spectrometer. Only two chambers are needed to give position and angle information about particle trajectories, but a third serves to increases the overall detection efficiency. Three plastic scintillators back the three wire chambers and form a trigger and timing signal for the HDC's. The intrinsic position resolution of each HDC is 174$\pm$9 μm [24, 27]. The chambers are placed 12.1 cm apart. This yields a worst case angular resolution of 1.37$\pm$ 0.07 mr. The focal plane instrumentation will be described in greater detail in a forthcoming report [26].

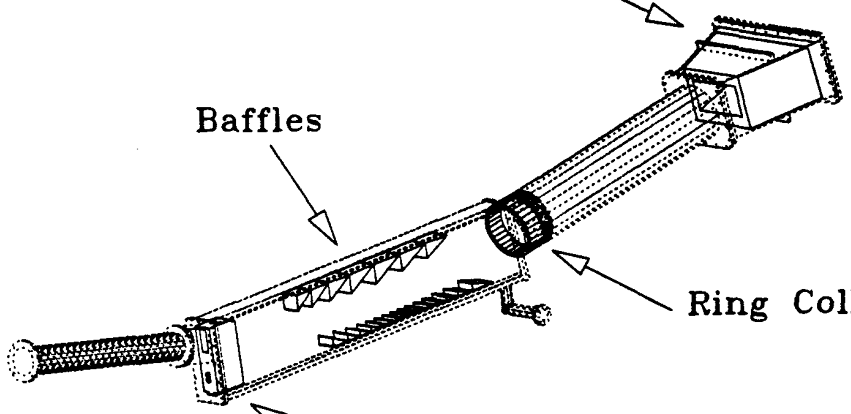

Figure 19: A view of the OOPS module vacuum system showing collimation.

5 Tolerances

The advantages of STAM, which permit the separation of structure function information from relative asymmetries and provide for substantial reductions in systematic errors, can be realized only if the OOPS modules are accurately positioned and aligned [3]. Angular coordinates (pointing) define both the independent dynamical variable (θ_{pq}) and the lever arm for separating the structure functions (ϕ_{pq}). The determination of these coordinates depends on the precise alignment of the OOPS module and its sub-systems as well as on a stable optical calibration.

Two distinct kinds of alignment errors can be defined:

1. Internal misalignments: relative errors in the placement of the magnets, trunnions, aperture defining collimators, and detectors internal to an OOPS module.
2. External misalignments: misalignment of the entire module with respect to the scattering plane, the target, and the other OOPS modules. Such misalignments reflect

uncertainties in the pointing of the central trajectory, the roll about the central trajectory, and the initial drift distance from the target.

Proper internal alignment is required to establish the integrity of the optical design and to maintain the calibration of the spectrometer. The mechanical structure of the OOPS module described in Section 4 is designed to fix the relative positions of the constituent elements independent of the orientation of the spectrometer. In principle, the degrees of freedom associated with internal alignments need to be adjusted once when the spectrometer is assembled. Afterward, only an appropriate external alignment of the spectrometer module is necessary to achieve the required performance. Specific external-alignment procedures will depend on the requirements of particular experiments and on the way in which the OOPS four-module cluster is supported in the experimental hall. This latter will be the subject of a future report.

The code TRANSPORT can be used to study the effect that translating or rotating an individual magnetic element has on the transfer matrix which describes the performance of the spectrometer. Corresponding errors in the determination of initial kinematic quantities can be estimated by multiplying focal-plane coordinate uncertainties by the inverted first order matrix.

With regard to internal misalignments, we note that the spectrometer calibration process determines the actual transfer matrix for a particular module. The two main concerns are first, that the initial assembly of the module reflects the design configuration with sufficient precision, and second, that the assembled module is rigid enough to maintain its optical integrity during subsequent relocations of the spectrometer as a whole. The orientation of the quadrupole with respect to the central ray is the most critical consideration. Table 5 shows that small translations in X and rotations in θ can effect the determination of both the scattering angle and the momentum. The orientation of the dipole is much less critical. After careful consideration, it was established that an assembly accuracy of ± 1 mm in the

Target Coords.	Misalignments						Cum. errors
	X ±0.5 mm	θ ±1.0 mr	Y ±0.5 mm	ϕ ±1.0 mr	Z ±0.5 mm	ψ ±1.0 mr	
θ_{target} (mr)	–0.43	–0.31	0.00	0.00	0.00	0.00	0.53
Y_{target} (cm)	0.00	0.00	–0.31	–0.23	0.00	0.00	0.38
ϕ_{target} (mr)	0.00	0.00	0.87	0.65	0.00	0.00	1.08
δ (%)	0.29	0.19	0.00	0.00	0.00	0.00	0.35

Table 5: Target coordinate uncertainties from quadrupole magnet misalignments.

relative positions of the magnets would be a conservative constraint from the point of view of obtaining the design optical-performance. The mechanical structure of the module has been engineered to retain the relative positions of the elements of the spectrometer to better than ± 0.3 mm.

External-alignment tolerances are governed by the accuracy with which a spectrometer module must be positioned in order to ensure a given level of certainty in the kinematic coordinates derived from the optical calibration. The best resolution that can be obtained from a perfectly aligned OOPS module is limited by the optical transfer matrix and by the uncertainty with which the detector package can measure the focal-plane coordinates of the particle trajectories. If energy losses and multiple scattering in the target and in the vacuum and detector windows are also included, this resolution is further reduced. Table 6 presents estimates of the uncertainties in the reconstruction of the kinematic coordinates by the OOPS module for a 1 mm-thick target. The results listed in column 2 reflect the spectrometer optics and the resolution of the detector package, while those in column 3 include multiple scattering effects as well. We note that these intrinsic uncertainties are well within the design specifications of section 2.

It is of interest to compare the magnitudes of the uncertainties in the reconstructed coordinates that arise from an external misalignment of the OOPS module to the intrinsic resolution limits of Table 6. Contributions to the uncertainties in the kinematic coordinates, corresponding to individual orthogonal translational errors of ± 1.0 mm and rotational errors of ± 0.5 mr in the placement of the module, are summarized in Table 7. If the spectrometer

	Target coordinate resolution	
	Intrinsic	Multiple Scattering
θ_{target} (mr)	0.57	2.9
Y_{target} (cm)	1.25	3.3
ϕ_{target} (mr)	3.15	3.5
δ (%)	0.15	0.26

Table 6: Intrinsic resolutions corresponding to a target size of 0.1 mm, without and with multiple scattering [11].

Target Coords.	Misalignments						Cum. errors
	X ±1.0 mm	θ ±0.5 mr	Y ±1.0 mm	ϕ ±0.5 mr	Z ±1.0 mm	ψ ±0.5 mr	
θ_{target} (mr)	–0.85	–1.40	0.00	0.00	–0.14	0.00	1.65
Y_{target} (cm)	0.00	0.00	–0.59	–0.97	0.00	0.11	1.14
ϕ_{target} (mr)	0.00	0.00	1.62	2.72	0.00	–0.23	3.17
δ (%)	0.55	0.92	0.00	0.00	0.17	0.00	1.08

Table 7: Target coordinate uncertainties from module misalignments.

can be located overall to ± 1.0 mm, and pointed to ± 0.5 mr, then the orientation uncertainties tabulated in Table 7 will be of the same order as the intrinsic uncertainties of Table 6, and the momentum resolution will be about 1 percent. It is clear that the ± 1.0 mm, ± 0.5 mr tolerance requirements place a significant constraint on the design of the support system for the four OOPS modules. However, particular experimental applications may make weaker resolution demands, and be accommodated with less stringent position tolerance limits.

The stability of the magnetic fields of the spectrometer will also contribute to uncertainties in the reconstructed coordinates. These uncertainties can be examined by studying the effects that changes in the dipole and quadrupole field strengths have on the first-order transfer matrix elements. The intrinsic resolution of the spectrometer as shown in Table 6 can be used to put an upper bound on the permissable variation in the magnetic field integral over the length of the particle trajectories. Maximum tolerable variations $\Delta B/B$ are summarized in Table 8. It is clear that if long term regulation on the order of 0.1 percent can be obtained, field stability will not present a problem.

Magnet	$\Delta B/B$				
	δ limited	θ limited	y limited	ϕ limited	Minimum
Dipole	2.06E–03	2.37E–03	1.29E–02	9.03E–03	2.06E–03
Quadrupole	1.01E–02	6.72E–03	0.43	0.10	6.72E–03

Table 8: Magnetic field tolerances.

6 Summary

In this report, we have described the ion-optical and physical design of a magnetic spectrometer that has been specifically tailored to perform out-of-plane coincidence $(e, e'p)$ measurements. Four such spectrometers, together with a support system which permits them to be arrayed azimuthally about a symmetry axis in the scattering plane, will comprise an out-of-plane spectrometer (OOPS) cluster. The instrument has been optimized for high precision measurements on the nucleon and on few body nuclear systems. A prototype spectrometer module has been constructed, and its performance characteristics are reported in a companion paper.

7 Acknowledgements

We would like to thank D. Biron, K.I. Blomqvist, S. Kowalski and C. Williamson for several useful discussions, and our consulting engineer, B. Bailey, for help with the mechanical design. This work was supported in part by the National Science Foundation under grant NSF PHY 89–21146 and the U. S. Department of Energy under contract # DE–ACO2–76ERO3069.

References

[1] S. Boffi, C. Giusti, and F. D. Pacati, Nuclear Physics **A435**, 697 (1985).

[2] G. Co, A. M. Lallena, and T. W. Donnelly, Nuclear Physics **A469**, 684 (1987).

[3] C. N. Papanicolas *et al.*, Nuclear Physics **A497**, 509c (1989).

[4] S. M. Dolfini, Ph.D. thesis, University of Illinois at Urbana-Champaign, 1993.

[5] J. B. Mandeville, Ph.D. thesis, University of Illinois at Urbana-Champaign, 1993.

[6] S. M. Dolfini *et al.*, Internal report, University of Illinois at Urbana-Champaign (unpublished).

[7] IFK Mainz Jahresbericht, Mainz, 1986–87, p. 103.

[8] Research Program at CEBAF, Vol.III CEBAF, VA, 1988, p. 183.

[9] STAR Spectrometer Conceptual Design Summary (October 1989), 1989, NPL Technical report No. 89–66.

[10] C. N. Papanicolas, in *Topical Conference on Electronuclear Physics with Internal Targets*, edited by R. G. Arnold (World Scientific Publishing Company, Stanford Linear Accelerator Center, Stanford, California, 1989), pp. 132–139.

[11] J. B. Mandeville *et al.*, Internal report, University of Illinois at Urbana-Champaign (unpublished).

[12] Research Proposal to the Bates Linear Accelerator Center; *"Measurement of the Quadrupole Contribution to the $N \rightarrow \Delta$ Excitation"*, 1987, Experiment #87–09.

[13] Research Proposal to the Bates Linear Accelerator Center; *"A Program to Determine the Five Deuterium* d(e,e'p) *Response Functions* ($R_L, R_T, R_{LT}, R_{TT}, R'_{LT}$)*"*, 1989, Experiment #89–14.

[14] Research Proposal to the Bates Linear Accelerator Center; *"Measurement of the* ($\vec{e}$, e'p) *Electrodisintegration of the Deuteron"*, 1989, Experiment #89–10.

[15] Fermi National Accelerator Laboratory, Fermilab Electron Cooling Experiment, 1978, Design Report.

[16] Accelerator Theory and Simulation Group, AT–6, *POISSON/SUPERFISH Group of Codes*, Los Alamos National Laboratory, Los Alamos, New Mexico, 1987, LA-UR–87–115 and LA-UR–87–126.

[17] Pacific Electric Motor Company Report, 1964.

[18] M. Garçon, *Private communication*, 1988.

[19] K. L. Brown, D. C. Carey, C. Iselin, and F. Rothacker, *TRANSPORT: A Computer Program for Designing Charged Particle Beam Transport Systems*, Stanford Linear Accelerator Center, 1991, SLAC–91, NAL–91, and CERN–73–16.

[20] J. E. Spencer and H. A. Enge, Nuclear Instruments and Methods **49**, 181 (1967).

[21] H. A. Enge and S. B. Kowalski, 3^{rd} International Conference on Magnet Technology, 1970, p. 103.

[22] D. C. Carey, *TURTLE (Trace Unlimited Rays Through Lumped Elements): A Computer Program For Simulating Charged Particle Beam Transport Systems*, Fermilab National Accelerator Laboratory, 1978, NAL–64.

[23] M. Farkhondeh, OOPS Internal Report, Bates Linear Accelerator Center (unpublished).

[24] L. G. Atencio, J. F. Amann, R. L. Boudrie, and C. L. Morris, Nuclear Instruments and Methods **187**, 381 (1981).

[25] A. H. Walenta, Nuclear Instruments and Methods **151**, 461 (1978).

[26] D. Jordan *et al.*, Internal report, Bates Linear Accelerator Center (unpublished).

[27] D. Toback, S.B. thesis, MIT, 1991.